Reprinted from The Journal of Physical Chemistry, **1989**, *93*, 2266.

Free Jet-Cooled Laser-Induced Fluorescence Spectrum of Methoxy Radical. 2. Rotational Analysis of the $\tilde{A}^2A_1 \longleftrightarrow \tilde{X}^2E$ Electronic Transition

Xianming Liu, Cristino P. Damo, Tai-Yuan David Lin, Stephen C. Foster,*,† Prabhakar Misra, Lian Yu, and Terry A. Miller

Laser Spectroscopy Facility, Department of Chemistry, The Ohio State University, 120 West 18th Avenue, Columbus, Ohio 43210 *(Received: May 24, 1988)*

The rotational structure of the 0_0^0 and 3_0^1 bands of the $\tilde{A}^2A_1 \leftrightarrow \tilde{X}^2E$ electronic transition of the methoxy radical has been measured. Simultaneous least-squares fits to these data and that from previously reported microwave studies of the ground state have been performed. Twelve molecular parameters for the ground state and six for the excited state, characterizing the rotational and spin structure of methoxy, have been determined. A brief discussion of the implications, in terms of geometries and electronic structure, of these parameters is given.

I. Introduction

The methoxy radical CH_3O is one of the most interesting of all free radicals. This fact is attested to by the over 75 papers that have been written "recently" about this species.[1] The interest is generated in at least two distinct ways. CH_3O is known to be a key intermediate in a number of extremely important chemical reactions. For example, it is a free radical formed in the combustion of hydrocarbon fuels. Add to that the role it plays in atmospheric reactions and its existence in interstellar space, and the study of its spectroscopy can easily be justified by the application of that spectroscopy to the elucidation of methoxy dynamics.

On the other hand, methoxy represents a classic spectroscopic challenge. It has an electronically degenerate ground state, ^2E, and hence is subject to Jahn–Teller distortion and a concomitant "quenching" of its electronic angular momentum with a corresponding diminution in its spin–orbit splitting. While Jahn–Teller effects are of a vibronic origin, the rotational levels, or rovibronic structure, should also be profoundly affected. Considerable theoretical work[2-6] has been expended upon the rovibronic

† Present address: Department of Chemistry, Florida State University, Tallahassee, FL 32306.

(1) See, for example, the reference given in the following: Brossard, S. D.; Carrick, P. G.; Chappell, E. L.; Hulegaard, S. C.; Engelking, P. C. *J. Chem. Phys.* **1986**, *84*, 2459.
(2) Child, M. S.; Longuet-Higgins, H. C. *Philos. Trans. R. Soc. London, A* **1961**, *254*, 259.
(3) Child, M. S. *Mol. Phys.* **1962**, *5*, 391; *J. Mol. Spectrosc.* **1963**, *10*, 357.
(4) Brown, J. M. *Mol. Phys.* **1971**, *20*, 817.
(5) Hougen, J. T. *J. Mol. Spectrosc.* **1980**, *81*, 73.

0022-3654/89/2093-2266$01.50/0

structure of degenerate electronic states, but there has been sparse experimental data for comparison. The paucity is particularly acute for molecules whose vibronic features are reasonably well-known and hence offer the opportunity for the most stringent comparisons of theory and experiment.

In our laboratory there has been a concerted effort to obtain a combination of vibronic and rovibronic data on several molecules with electronically degenerate and near-degenerate ground states. The species whose vibronic and rovibronic structure have been studied experimentally include methoxy, CH_3O, monomethyl sulfide, CH_3S, cyclopentadienyl, C_5H_5, and the halobenzene cations $C_6F_6^+$ and *sym*-$C_6H_3F_3^+$. These species taken as a group offer an excellent ensemble for study as they differ markedly in size, shape, and atomic composition. For example, in the group we already know that spin–orbit splittings vary from $>10^2$ cm^{-1} to unmeasurably small.

The present paper on methoxy is the second of several that will deal with this radical. Recently we[7] have reported a detailed analysis of the vibronic structure of both the $\tilde{A}^2A_1$ and the $\tilde{X}^2E$ states of methoxy. Indeed, it might seem, that with all the attention paid to methoxy, there would be little left to learn. The ground-state rovibronic structure has been studied extensively by laser magnetic resonance (LMR)[8] and microwave[9] techniques. Our approach involves high-resolution optical spectroscopy of the $\tilde{A}^2A_1 \leftrightarrow \tilde{X}^2E$ transition of jet-cooled CH_3O. Interestingly, there has been no previous detailed analysis of any rotationally resolved optical spectrum of methoxy. (Note, however, the pioneering work of Powers et al.[10] and also that of Fuke et al.[11]) Thus our experiment can be expected to yield the first precise rotational parameters for the excited $\tilde{A}$ state. Such parameters are of considerable interest because of the strong theoretical interest[12-16] in the structure of both the $\tilde{A}$ and $\tilde{X}$ states. However, rather surprisingly, our results are also able to somewhat improve the ground-state rotational parameters for CH_3O. This is possible since even though the microwave data, in particular, are much more precise, the optical transitions determine directly the relative positions of ground-state energy levels only indirectly determined in the earlier studies. These ground- and excited-state rotational parameters and a discussion of their implications are the principal result of this present work.

II. Experimental Section

The experimental apparatus and procedures were very similar to those reported in ref 7 and will not be detailed here. As before CH_3O was produced by KrF excimer laser photolysis of methyl nitrite seeded into a He supersonic free jet expansion. The rotationally resolved excitation spectra of the 0_0^0 and 3_0^1 bands were obtained by using the frequency-doubled output of a XeCl excimer pumped dye laser (respectively Lumonics Excimer-510 and Hyperdye-300). Typically this combination produced ≈0.5 mJ/pulse of UV light, which could be tuned in an automated manner over ≈500 cm^{-1}.

Frequency calibration was accomplished by simultaneously recording the I_2 spectrum with the laser fundamental while observing the CH_3O spectrum with its doubled output. The precise positions of the CH_3O lines are obtained by the following procedure. A computer program is used to obtain the positions of both the I_2 and CH_3O lines in terms of the dye laser grating counter position. With the I_2 atlas,[17] this procedure yields precisely known frequencies for a large number of grating positions. The frequency of the laser at any grating position can be expressed as accurately as needed via a power series relationship between the frequency and the grating counter reading. A least-squares fit of the I_2 frequencies gives us the coefficients of a third-order polynomial relationship. The absolute frequencies of the methoxy lines are then found from their grating counter positions by using the polynomial relation. The standard deviation in the fit to the I_2 lines is always less than 0.03 cm^{-1}. The consistency among absolute frequencies of given methoxy lines of different data sets is ≲0.04 cm^{-1}, about one-fifth the line width of the doubled dye laser.

III. Theory

The theory of a rotationally resolved electronic transition, even one involving a degenerate electronic state, is well developed[18] and normally would need little elaboration. However, special attention must be paid to two points. We also wish to make use of the high-resolution microwave results,[9] already available for the ground ^2E state. We will accomplish this by performing a least-squares fits to a suitably weighted combination of the microwave and optical data. Thus our depiction of the ground-state levels must be precise to the accuracy of the microwave data, of the order of 10 kHz. Fortunately we can follow much of the work of Endo et al.[9] in this respect. However, we also wish to develop the rotational analysis in a manner most suitable for a later comparison with the analysis of the Jahn–Teller perturbed vibronic energy levels. For this reason we will briefly review the theory underlying the "rotational" structure of both the ground ^2E and excited ^2A states.

A. Ground ^2E State. The rovibronic structure of doublet E electronic states has received considerable attention. Child and Longuet-Higgins[2] laid the theoretical framework, which was enlarged upon by Child[3] and then by Brown[4] and Russell and Radford[8] and group theoretically consummated by Hougen.[5] This approach has been applied to an analysis of the microwave spectrum of CH_3O by Endo et al.[9] A parallel development has been given by Watson.[6]

Let us define the rotational angular momentum, **R**:

$$\mathbf{R} = \mathbf{J} - \mathbf{S} - \mathbf{L} - \mathbf{G} \tag{1}$$

where **J** is the total angular momentum exclusive of nuclear spin,[19] **L** is the electronic orbital angular momentum, **S** is the electronic spin angular momentum, and **G** is the vibrational angular momentum.

If we make no assumptions about the molecular geometry, one can always write[5,6] the rigid-body rotational Hamiltonian as

$$\mathcal{H}_R = \tfrac{1}{2}\sum_{i,j} R_i I_{ij}^{-1} R_j \tag{2}$$

where the I_{ij}^{-1}'s are the elements of the inverse of the inertial tensor and i and j run over the Cartesian coordinates x, y, and z.

To proceed further, we need to choose a basis set. The simplest appropriate function (exclusive of nuclear spin[19]) can be written

$$|(\Lambda,v_j,l_j,\mathbf{j}),\alpha,J,P,M,S,\Sigma\rangle = |(\Lambda,v_j,l_j,\mathbf{j}),\alpha\rangle|J,P,M\rangle|S,\Sigma\rangle \tag{3}$$

On the left-hand side, the vibronic key may be assumed to be a linear combination of the eigenfunction kets for the vibronic problem. In a degenerate electronic state with Jahn–Teller dis-

(6) Watson, J. K. G. *J. Mol. Specrosc.* **1984**, *103*, 125.
(7) Foster, S. C.; Misra, P.; Lin, T.-Y.; Damo, C. P.; Carter, C. C.; Miller, T. A. *J. Phys. Chem.* **1988**, *92*, 4263.
(8) Radford, H. E.; Russell, D. K. *J. Chem. Phys.* **1977**, *66*, 2222. Russell, D. K.; Radford, H. E. *J. Chem. Phys.* **1980**, *72*, 2750.
(9) Endo, Y.; Saito, S.; Hirota, E. *J. Chem. Phys.* **1984**, *81*, 122.
(10) Powers, D. E.; Hopkins, J. B.; Smalley, R. E. *J. Phys. Chem.* **1981**, *85*, 2711.
(11) Fuke, K.; Ozawa, K.; Kaya, K. *Chem. Phys. Lett.* **1986**, *126*, 119.
(12) Yarkony, D. R.; Schaefer, H. F., III; Rothenberg, S. *J. Am. Chem. Soc.* **1974**, *96*, 656.
(13) Ohkubo, K.; Fujita, T.; Sato, H. *J. Mol. Struct.* **1977**, *36*, 101.
(14) Bent, G. D.; Adams, G. F.; Bartram, R. H.; Purvis, G. D.; Bartlett, R. J. *J. Chem. Phys.* **1982**, *76*, 4144.
(15) Jackels, C. F. *J. Chem. Phys.* **1982**, *76*, 505.
(16) Saebø, S.; Radom, L.; Schaefer, H. F., III. *J. Chem. Phys.* **1983**, *78*, 845.
(17) Gerstenkorn, S.; Luc, P. *Atlas du Spectre d'absorption de la Molecule d'Iode*; Centre National de la Recherche Scientifique: Paris, 1978. See also: Gerstenkorn, S.; Luc, P. *Rev. Phys. Appl.* **1979**, *14*, 791.
(18) See, for example: Herzberg, G. *Electronic Spectra of Polyatomic Molecules*; Van Nostrand: New York, 1966.
(19) It is completely permissible for our purposes to consider the nuclear spin-free Hamiltonian even though Endo et al.[9] observed hyperfine structure in the microwave methoxy spectrum. For our analysis we use their "hyperfine-free" frequencies (Table III of ref 9), and hyperfine splittings are unresolved in the optical spectrum, for which, of course, nuclear spin statistics are included in the intensity calculations.

tortion, such kets can rigorously be characterized only by the irreducible representations, e, a, etc., according to which they transform as is indicated by the quantum number α. The combination of approximate quantum numbers (Λ,v_j,l_j,j) then serve as a convenient index distinguishing among those functions with the same value of α. The ket $|J,P,M\rangle$ corresponds to the "rotational" wave function with P and M being respectively the projection of J along the molecule-fixed and space-fixed z axis. The electronic spin ket $|S\Sigma\rangle$ gives the value, Σ, of the molecule fixed projection of S. To describe the rotational spectrum of an E state, Endo et al.[9] found it most convenient to take the symmetric and antisymmetric combination of the functions of opposite signs of the molecule fixed-projection, i.e.

$$|(\Lambda,v_j,l_j,j),\alpha,J,P,M,S,\Sigma,\pm\rangle = 2^{-1/2}[|(\Lambda,v_j,l_j,j),\alpha,J,P,M,S,\Sigma\rangle \pm (-1)^{J-P+S-\Sigma}|(-\Lambda,v_j,-l_j,-j),\alpha,J,-P,M,S,-\Sigma\rangle] \quad (4)$$

where now the quantum numbers Λ and l_j on the left-hand side of the equals sign take on only magnitudes and not signed values, but P takes on all values $P = J, J-1, \ldots, -J$ and $\Sigma = S, S-1, \ldots, -S$. The linear combination with Λ and Σ of the same sign corresponds to the $^2E_{3/2}$ state, while the $^2E_{1/2}$ state is represented by the linear combination with Λ and Σ of different signs.

If we use eq 4 to take an expectation value of eq 2, we can construct an effective rotational Hamiltonian, $\mathcal{H}^R$, for the E state as

$$\mathcal{H}^R = \sum_{i=1}^{4} \mathcal{H}_i^R \quad (5)$$

with

$$\mathcal{H}_1^R = A[(J_z - S_z)^2 - 2A(\xi_t - \epsilon/A)(J_z - S_z)] + B(\mathbf{J}^2 - J_z^2) \quad (6)$$

$$\mathcal{H}_2^R = -2B[J_xS_x + J_yS_y] \quad (7)$$

$$\mathcal{H}_3^R = h_1(\mathbf{L}_-^2J_+^2 + \mathbf{L}_+^2J_-^2) + h_2[\mathbf{L}_-^2(J_zJ_- + J_-J_z) + \mathbf{L}_+^2(J_zJ_+ + J_+J_z)] - 2h_2(\mathbf{L}_-^2J_-S_z + \mathbf{L}_+^2J_+S_z) \quad (8)$$

$$\mathcal{H}_4^R = -2h_1(\mathbf{L}_-^2J_+S_+ + \mathbf{L}_+^2J_-S_-) - 2h_2(\mathbf{L}_-^2J_zS_- + \mathbf{L}_+^2J_zS_+) \quad (9)$$

Terms constant for the vibronic level have been omitted from $\mathcal{H}^R$. The molecular parameters appearing in $\mathcal{H}^R$ are defined in terms of matrix elements over the vibronic eigenfunctions (including Jahn–Teller effects):

$$A = \tfrac{1}{2}\langle e_\pm|I_{zz}^{-1}|e_\pm\rangle \quad (10a)$$

$$B = \tfrac{1}{4}\langle e_\pm|I_{xx}^{-1} + I_{yy}^{-1}|e_\pm\rangle \quad (10b)$$

$$h_1\mathbf{L}_\pm^2 = \tfrac{1}{8}\langle e_\pm|I_{xx}^{-1} - I_{yy}^{-1} \pm 2iI_{xy}^{-1}|e_\mp\rangle \quad (11a)$$

$$h_2\mathbf{L}_\mp^2 = \tfrac{1}{4}\langle e_\mp|I_{zx}^{-1} \pm iI_{zy}^{-1}|e_\pm\rangle \quad (11b)$$

$$A\xi_t = \pm\langle e_\pm|I_{zz}^{-1}(L_z + G_z)|e_\pm\rangle \quad (12a)$$

$$\epsilon = \pm\tfrac{1}{4}\langle e_\pm|(L_- + G_-)(I_{zx}^{-1} + iI_{zy}^{-1}) + (L_+ + G_+) \times (I_{zx}^{-1} - iI_{zy}^{-1})|e_\pm\rangle \quad (12b)$$

The kets $|e_\pm\rangle$ symbolize the appropriate linear combination of functions $|(\Lambda=\pm1,v,l,j),\alpha\rangle$ which is the vibronic eigenfunction for the ground state, i.e., nominally $\Lambda = \pm1$, $v = 0$, $l = 0$, $j = {}^1/_2$, and $\alpha = e_\pm$. As noted above, only α is a good quantum number. $\mathbf{L}_\pm^2$ is the artificial ladder operator introduced by Hougen which converts $e_\pm$ into $e_\mp$ in C_{3v} symmetry.

Written in this fashion, each of the terms of $\mathcal{H}^R$ has a simple physical significance. The first term, $\mathcal{H}_1^R$, is the combined Hamiltonian for rotational motion, electronic spin, and orbital Coriolis interaction for a symmetric top molecule. It has only diagonal matrix elements in the Hund's case a like basis set of eq 4. $\mathcal{H}_2^R$ yields the spin uncoupling effects with nonvanishing matrix elements connecting the $^2E_{3/2}$ and $^2E_{1/2}$ states.

The remaining two terms, $\mathcal{H}_3^R$ and $\mathcal{H}_4^R$, of $\mathcal{H}^R$ yield the effects upon the rotational energy levels caused by the Jahn–Teller vibrational–electronic interaction. $\mathcal{H}_3^R$ contains only operators connecting the $^2E_{1/2}$ and $^2E_{3/2}$ states. $\mathcal{H}_4^R$ contains only operators with nonvanishing maatrix elements only within the $^2E_{1/2}$ state (first term) or the $^2E_{3/2}$ state (second term). Hougen notes that for small distortions (with certain other restrictions) that

$$\epsilon \approx 0 \quad (13)$$

Clearly for a rigid symmetric top nondegenerate state h_1 and h_2 both vanish.

Both Hougen and Watson have pointed out that the parameters in $\mathcal{H}^R$ are not completely defined by expectation values over the vibronic eigenfunction, eq 10–12. There exist besides operators connecting the ^2E state of interest to other electronic states. The effect of these couplings upon the rotational energy levels of the ^2E state are likely to be quite small. Nonetheless, in essence any parameter, P, in $\mathcal{H}^R$ (including h_1 and h_2) should be represented as a sum of two terms, i.e.

$$P = P^v + P^L \quad (14)$$

where P^v represents the expectation value of which we have spoken above and P^L represents a correction due to L uncoupling. Both Watson and Hougen have given explicit expressions for the P^L's valid through second-order perturbation theory.

The corrections P^L to the standard rotational constants, A, B, etc., have been long known and are quite small for any molecule for which the Born–Oppenheimer approximation is reasonably valid. If the molecule suffers a significant Jahn–Teller effect, the contributions P^L to h_1 and h_2 are similarly small compared to the Jahn–Teller contribution represented by P^v.

Up to this point we have not considered explicitly the effects of electron spin coupling to its orbital motion or the rotation of the molecule. As long as we are concerned only with an effective operator within a ^2E state, the spin–orbit coupling operator can be represented by

$$\mathcal{H}^{SO} = a\mathbf{L}\cdot\mathbf{S} \quad (15)$$

Van Vleck[20] showed long ago that the general form of the spin–rotation interaction can be written

$$\mathcal{H}^{SR} = a_0\mathbf{R}\cdot\mathbf{S} + a(3R_zS_z - \mathbf{R}\cdot\mathbf{S}) + b(R_xS_x - R_yS_y) + c(R_xS_y + R_yS_x) + d(R_xS_z + R_zS_x) + e(R_yS_z + R_zS_y) \quad (16)$$

where the coefficients a_0 and a–e were unspecified but known to consist of both first- and second-order contributions analogous to the rotational parameters, P, as illustrated by eq 14.

It is relatively easy to show that $\mathcal{H}_{SR}$ can be written as

$$\mathcal{H}^{SR} = \mathcal{H}_{ST}^{SR} + \mathcal{H}_D^{SR} \quad (17)$$

where $\mathcal{H}_{ST}^{SR}$ denotes the terms present for a nondegenerate symmetric top and $\mathcal{H}_D^{SR}$ indicates the remaining not necessarily vanishing terms corresponding to the expectation value of the vibronic eigenfunction. Following Hougen and adopting his notation give

$$\mathcal{H}_{ST}^{SR} = \epsilon_{aa}R_zS_z + \tfrac{1}{4}(\epsilon_{bb} + \epsilon_{cc})(R_+S_- + R_-S_+) \quad (18)$$

from the first two terms of eq 16. From the remaining terms of eq 16 we obtain

$$\mathcal{H}_D^{SR} = \epsilon_1(\mathbf{L}_-^2R_+S_+ + \mathbf{L}_+^2R_-S_-) + \epsilon_{2a}[\mathbf{L}_-^2(R_zS_- + S_-R_z) + \mathbf{L}_+^2(R_zS_+ + S_+R_z)] + \epsilon_{2b}[\mathbf{L}_-^2(R_-S_z + S_zR_-) + \mathbf{L}_+^2(R_+S_z + S_zR_+)] \quad (19)$$

The ϵ_{ij} and $\mathbf{L}_\pm^2$ (see eq 11a and 11b) are operators within the vibronic manifold, and so their expectation values correspond to vibronic-level-dependent parameters for the spin interactions.

There are, of course, also contributions to the energy due to second-order (and higher) contributions from excited vibronic

(20) Van Vleck, J. H. *Rev. Mod. Phys.* **1951**, *23*, 213.
(21) DeSantis, D.; Lurio, A.; Miller, T. A.; Freund, R. S. *J. Chem. Phys.* **1973**, *58*, 4625.

levels. These terms are usually taken into account through a centrifugal distortion Hamiltonian, $\mathcal{H}_{CD}$. Thus we write our total Hamiltonian as

$$\mathcal{H} = \mathcal{H}_0 + \mathcal{H}_{CD} \tag{20}$$

where

$$\mathcal{H}_0 = \mathcal{H}^R + \mathcal{H}^{SO} + \mathcal{H}^{SR} \tag{21}$$

and we follow Endo et al.[9] in writing

$$\mathcal{H}_{CD} = a_D R_z^2 L_z S_z + \eta_e \mathbf{R}^2 R_z (L_z + G_z) + \eta_K R_z^3 (L_z + G_z) - D_N \mathbf{R}^4 - D_{NK} \mathbf{R}^2 R_z^2 - D_K R_z^4 + (h_{1N}/2)[\mathbf{R}^2, \mathbf{L}_-^2 R_+^2 + \mathbf{L}_+^2 R_-^2]_+ + (h_{1K}/2)[R_z^2, \mathbf{L}_-^2 R_+^2 + \mathbf{L}_+^2 R_-^2]_+ + (h_{2N}/2)[\mathbf{R}^2, \mathbf{L}_-^2 (R_z R_- + R_- R_z) + \mathbf{L}_+^2 (R_z R_+ + R_+ R_z)]_+ + (h_{2K}/2)[R_z^2, \mathbf{L}_-^2 (R_z R_- + R_- R_z) + \mathbf{L}_+^2 (R_z R_+ + R_+ R_z)]_+ + h_4 (\mathbf{L}_-^2 R_-^4 + \mathbf{L}_+^2 R_+^4) \tag{22}$$

The matrix elements of the total Hamiltonian, eq 20, have been determined in the basis set, eq 4, by Endo et al.,[9] and we have used their results. In evaluating $\mathcal{H}^{SR}$ and $\mathcal{H}_{CD}$ they have approximated $\mathbf{R}$ by $\mathbf{J} - \mathbf{S}$ rather than $\mathbf{J} - \mathbf{S} - \mathbf{L} - \mathbf{G}$. However, since $\mathbf{L} + \mathbf{G}$ has only constant matrix elements in the vibronic state of interest (or ones connecting it to other vibronic states) for these smaller Hamiltonian terms, this is a reasonable procedure.

B. $\tilde{A}^2A$ Excited State. The rotational structure of the $^2A_1$ excited state is, of course, much simpler than for the ^2E state. As long as we deal with excitation to any totally symmetric vibrational level of the $\tilde{A}$ state, we need not concern ourselves with any nonzero expectation values of either the electronic or vibrational angular momentum. Furthermore in these experiments, no electron spin splittings were resolved in the $\tilde{A}$ state. Thus we can take $\mathcal{H}_0$ as eq 21 and reduce it:

$$\mathcal{H}_0 = \mathcal{H}^R + \mathcal{H}^{SO} + \mathcal{H}^{SR} = \mathcal{H}^R = \mathcal{H}_1^R = B_v \mathbf{N}^2 + (A_v - B_v) N_z^2 + \nu_{vo} \tag{23}$$

Since the molecule is close to Hund's case b, we introduce the conserved case **b** angular momentum, $\mathbf{N} = \mathbf{J} - \mathbf{S}$, with projection along the top axis of K. We introduce the subscript v on the parameters to indicaate that as usual they are functions of the vibrational level over which the usual expectation values, analogous to eq 10–12, are to be taken. The parameter ν_{vo} is introduced to denote the vibronic energy of the appropriate ν_3 level of the $^2A_1$ state.

It is again necessary to add to $\mathcal{H}_0$ a centrifugal distortion term, $\mathcal{H}_{CD}$. However, its form is now much simpler and follows from eq 22:

$$\mathcal{H}_{CD} = -D_N \mathbf{N}^4 - D_{NK} \mathbf{N}^2 N_z^2 - D_K N_z^4 \tag{24}$$

A general, symmetrized case b basis function can be written[4]

$$|J=N\pm{}^1/_2,K,M_J,N,S,\pm\rangle = \sum_{M_S,M_N} (-1)^{N-S+M_J} (2J+1)^{1/2} \times \begin{pmatrix} N & S & J \\ M_N & M_S & -M_J \end{pmatrix} |N,K,M_N,\pm\rangle |SM_S\rangle \tag{25}$$

with

$$|N,K,M_N,\pm\rangle = 2^{-1/2}[|N,K,M_N\rangle \pm (-1)^{N-K} |N,-K,M_N\rangle] \quad (K \neq 0) \tag{26}$$

For $K = 0$, the simple ket $|N,K,M_N\rangle$ obviously suffices. Since in this work transitions to $J = N \pm {}^1/_2$ are degenerate and not distinguished, the Hamiltonian $\mathcal{H}_0 + \mathcal{H}_{CD}$ may be evaluated by using eq 25, yielding only diagonal values, i.e.

$$\langle \mathcal{H}_0 + \mathcal{H}_{CD} \rangle = B_v N(N+1) + (A_v - B_v) K^2 - D_N N^2 (N+1)^2 - D_{NK} N(N+1) K^2 - D_K K^4 + \nu_{vo} \tag{27}$$

C. Transition Intensities. It is important to consider the intensities of the laser-induced fluorescence (LIF) transitions in the $\tilde{A}^2A_1 \leftrightarrow \tilde{X}^2E$ electronic transition for two distinct reasons. First, the intensities play an important role in making and confirming particular assignments in the rotationally resolved spectrum. Second, it is of considerable interest to inquire as to whether the rotational levels of methoxy in the jet are in Boltzmann equilibrium and, if so, at what temperature.

In the LIF process, molecules absorb laser photons with frequency ν_l and polarization μ_l and are excited from initial level A to an excited level B, followed by emission of photons of frequency ν_f and polarization μ_f to a final level C. The fluorescence intensity in such a process is described by[22]

$$I(\mathrm{A,B,C};\mu_l\mu_f) = N_a^R \rho(\nu_l,\mu_l)\, \nu_f^3 K(\nu_f)\, S_{ab}(\alpha,\beta)\, S_{bc}(\beta,\gamma) \times \left\{ \sum_{M_b M_{b'}} (-1)^{M_b - M_{b'}} \sum_{M_a} F(M_a) \times \begin{pmatrix} J_a & 1 & J_b \\ -M_a & \mu_l & M_b \end{pmatrix} \begin{pmatrix} J_a & 1 & J_b \\ -M_a & \mu_l & M_{b'} \end{pmatrix} \times \sum_{M_c} G(\mu_F) \begin{pmatrix} J_b & 1 & J_c \\ -M_b & \mu_f & M_c \end{pmatrix} \begin{pmatrix} J_b & 1 & J_c \\ -M_b & \mu_f & M_c \end{pmatrix} \right\} \tag{28}$$

where $K(\nu_f)$ and $G(\mu_f)$ are the detector response as a function of frequency ν_f and polarization μ_f, respectively, $\rho(\nu_l,\mu_l)$ is the radiation density of the laser beam, N_a^R is the number of molecules in the initial rotational state, $S_{\alpha\beta}$ is the line strength of the transition $\alpha \rightarrow \beta$ calculated as if it takes place in isotropic free space, M_α is the projection of the total angular momentum $\mathbf{J}_\alpha$ on the space-fixed axis (z), and $F(M_a)$ is the fraction in the sublevel M_a. The parameters α, β, and γ denote all the quantum numbers (including J) needed to define a specific quantum level in the A, B, and C electronic states, respectively.

In our experiment, the laser is linearly polarized with its electric field vector along the z axis ($\mu_l = 0$) and the M_a sublevels of the initial state are assumed equally populated ($F(M_a)$ = constant). If the detector constant and frequency ν_f do not change significantly over the range of the emission frequencies, both $K(\nu_f)$ and ν_f can be considered as constants. Since the total fluorescence is collected, we should sum over all the possible final states and polarizations:

$$I(\mathrm{A,B}) = \sum_C (\mathrm{A,B,C}) = K N_a^R \rho(\nu_l)\, S_{ab}(\alpha,\beta) \sum_{M_b} \left\{ \begin{pmatrix} J_a & 1 & J_b \\ -M_b & 0 & M_b \end{pmatrix}^2 \times \sum_\gamma \left[\frac{1}{2}(1+\cos^2\theta) \begin{pmatrix} J_b & 1 & J_c \\ -M_b & -1 & M_b+1 \end{pmatrix}^2 + \sin^2\theta \begin{pmatrix} J_b & 1 & J_c \\ -M_b & 0 & M_b \end{pmatrix}^2 + \frac{1}{2}(1+\cos^2\theta) \times \begin{pmatrix} J_b & 1 & J_c \\ -M_b & 1 & M_b-1 \end{pmatrix}^2 \right] \times S_{bc}(\beta,\gamma) \right\} \tag{29}$$

where $K = K(\nu_f)\nu_f^3$ and is assumed to be a constant. The cosine and sine θ terms approximate $G(\mu_f)$ as the detector views only at an angle θ ($\theta = 0°$ in our experiment) with respect to the z axis. This approximation is tantamount to assuming that the detector itself is insensitive to the polarization of the photons but reflects the variation in abundance of photons as a function of angle that is inherent in polarized emission.

The key factors remaining in eq 29 are the isotropic transition probabilities S. We use ^2E state basis functions, $|E,J,P,M,S,\Sigma,\pm\rangle$, defined by eq 4 and ^2A state basis functions, $|A,J,M,N,K,S,\pm\rangle$ defined by eq 25 and 26. After a considerable amount of manipulation detailed in the Appendix, we obtain in eq A14 and A15 explicit expressions for the S's contained in eq 29.

The only remaining quantity requiring discussion is the population in a given rotational level N_a^R. If methoxy's rotational population is in thermal equilibrium, then for the E state

$$N_a^R = Z^{-1} N_E^T g_I e^{-E_R/kT} \tag{30}$$

(22) Kinsey, J. L. *Ann. Rev. Phys. Chem.* **1977**, *28*, 349.

TABLE I: Methoxy $\tilde{A}^2A_1 \rightarrow \tilde{X}^2E_{3/2}$ 0_0^0 Rotational Transitions

J''	K''^a	Σ''	$J_1'^b$	$J_2'^b$	K'	obsd, cm^{-1}	obsd − calcd
8.5	1.0	0.5	7.5		0.0	31613.66	0.02
7.5	2.0	0.5	6.5		1.0	31615.32	0.05
6.5	3.0	0.5	5.5		2.0	31616.52	0.05
8.5	3.0	0.5	8.5	7.5	2.0	31618.21	−0.07
7.5	1.0	0.5	6.5		0.0	31618.80	−0.02
6.5	2.0	0.5	5.5		1.0	31620.15	0.03
5.5	3.0	0.5	4.5		2.0	31620.97	−0.01
9.5	1.0	0.5	9.5	8.5	0.0	31621.40	0.07
7.5	3.0	0.5	7.5	6.5	2.0	31622.03	0.02
7.5	0.0	0.5	6.5		1.0	31622.27	0.06
5.5	2.0	0.5	4.5		1.0	31624.67	0.04
4.5	3.0	0.5	3.5		2.0	31625.14	0.00
7.5	2.0	0.5	7.5	6.5	1.0	31625.58	−0.08
6.5	0.0	0.5	5.5		1.0	31627.01	−0.05
5.5	1.0	0.5	4.5		0.0	31628.17	0.01
5.5	3.0	0.5	5.5	4.5	2.0	31628.40	−0.01
4.5	2.0	0.5	3.5		1.0	31628.80	0.02
8.5	0.0	0.5	8.5	7.5	1.0	31628.80	−0.09
3.5	3.0	0.5	2.5		2.0	31628.94	0.00
6.5	2.0	0.5	6.5	5.5	1.0	31628.94	−0.09
7.5	1.0	0.5	7.5	6.5	0.0	31629.23	0.09
4.5	3.0	0.5	4.5	3.5	2.0	31631.08	0.01
5.5	0.0	0.5	4.5		1.0	31631.59	0.04
5.5	2.0	0.5	5.5	4.5	1.0	31632.07	0.01
4.5	1.0	0.5	3.5		0.0	31632.32	0.01
3.5	2.0	0.5	2.5		1.0	31632.59	0.00
6.5	1.0	0.5	6.5	5.5	0.0	31632.59	0.07
7.5	0.0	0.5	7.5	6.5	1.0	31632.59	−0.01
3.5	3.0	0.5	3.5	2.5	2.0	31633.39	−0.00
4.5	2.0	0.5	4.5	3.5	1.0	31634.73	0.00
5.5	1.0	0.5	5.5	4.5	0.0	31635.63	0.07
4.5	0.0	0.5	3.5		1.0	31635.63	−0.07
2.5	2.0	0.5	1.5		1.0	31636.06	0.02
6.5	0.0	0.5	6.5	5.5	1.0	31636.06	0.10
3.5	1.0	0.5	2.5		0.0	31636.06	−0.04
3.5	2.0	0.5	3.5	2.5	1.0	31637.03	−0.01
4.5	1.0	0.5	4.5	3.5	0.0	31638.24	0.02
5.5	0.0	0.5	5.5	4.5	1.0	31638.98	0.01
2.5	2.0	0.5	2.5	1.5	1.0	31638.98	−0.03
2.5	1.0	0.5	1.5		0.0	31639.53	−0.01
3.5	0.0	0.5	2.5		1.0	31639.55	0.06
3.5	1.0	0.5	3.5	2.5	0.0	31640.55	0.00
5.5	2.0	0.5	6.5	5.5	1.0	31641.00	0.03
4.5	0.0	0.5	4.5	3.5	1.0	31641.67	0.03
4.5	2.0	0.5	5.5	4.5	1.0	31642.15	−0.01
2.5	1.0	0.5	2.5	1.5	0.0	31642.56	0.05
1.5	1.0	0.5	0.5		0.0	31642.56	−0.09
2.5	0.0	0.5	1.5		1.0	31642.94	0.00
6.5	1.0	0.5	7.5	6.5	0.0	31642.94	−0.02
3.5	2.0	0.5	4.5	3.5	1.0	31642.94	−0.04
2.5	2.0	0.5	3.5	2.5	1.0	31643.45	−0.02
1.5	1.0	0.5	1.5	0.5	0.0	31644.11	−0.02
5.5	1.0	0.5	6.5	5.5	0.0	31644.46	−0.03
4.5	−1.0	0.5	4.5	3.5	2.0	31644.97	0.02
4.5	1.0	0.5	5.5	4.5	0.0	31645.67	−0.00
2.5	0.0	0.5	2.5	1.5	1.0	31645.90	−0.01
3.5	1.0	0.5	4.5	3.5	0.0	31646.48	−0.02
2.5	1.0	0.5	3.5	2.5	0.0	31647.03	0.05
1.5	1.0	0.5	2.5	1.5	0.0	31647.03	−0.08
1.5	0.0	0.5	1.5	0.5	1.0	31647.53	0.00
5.5	0.0	0.5	6.5	5.5	1.0	31647.89	0.00
4.5	0.0	0.5	5.5	4.5	1.0	31649.07	0.01
2.5	−1.0	0.5	2.5	1.5	2.0	31649.17	−0.05
3.5	0.0	0.5	4.5	3.5	1.0	31649.90	0.01
0.5	0.0	0.5	1.5	0.5	1.0	31650.35	0.07
2.5	0.0	0.5	3.5	2.5	1.0	31650.41	0.04
1.5	0.0	0.5	2.5	1.5	1.0	31650.47	−0.03
7.5	−2.0	0.5	8.5	7.5	3.0	31651.10	0.02
5.5	−1.0	0.5	6.5	5.5	2.0	31651.20	−0.00
1.5	1.0	0.5		2.5	0.0	31651.52	−0.04
4.5	−1.0	0.5	5.5	4.5	2.0	31652.37	−0.01
2.5	1.0	0.5		3.5	0.0	31652.90	−0.02
6.5	−2.0	0.5	7.5	6.5	3.0	31652.90	−0.04
3.5	−1.0	0.5	4.5	3.5	2.0	31653.21	0.02
0.5	0.0	0.5		1.5	1.0	31653.21	−0.04
2.5	−1.0	0.5	3.5	2.5	2.0	31653.73	0.06
1.5	−1.0	0.5	2.5	1.5	2.0	31653.76	−0.04

TABLE I (Continued)

J''	K''^a	Σ''	$J_1'^b$	$J_2'^b$	K'	obsd, cm^{-1}	obsd − calcd
3.5	1.0	0.5		4.5	0.0	31 653.83	−0.08
5.5	−2.0	0.5	6.5	5.5	3.0	31 654.52	0.09
4.5	1.0	0.5		5.5	0.0	31 654.52	−0.04
1.5	0.0	0.5		2.5	1.0	31 654.92	−0.04
4.5	−2.0	0.5	5.5	4.5	3.0	31 655.60	0.00
2.5	0.0	0.5		3.5	1.0	31 656.35	0.04
3.5	−2.0	0.5	4.5	3.5	3.0	31 656.47	0.07
0.5	−1.0	0.5		1.5	2.0	31 656.54	0.00
2.5	−2.0	0.5	3.5	2.5	3.0	31 656.87	−0.00
3.5	0.0	0.5		4.5	1.0	31 657.31	−0.00
4.5	0.0	0.5		5.5	1.0	31 657.97	−0.00
1.5	−1.0	0.5		2.5	2.0	31 658.25	0.00
5.5	0.0	0.5		6.5	1.0	31 658.25	−0.03
2.5	−1.0	0.5		3.5	2.0	31 659.61	0.00
3.5	−1.0	0.5		4.5	2.0	31 660.60	−0.02
4.5	−1.0	0.5		5.5	2.0	31 661.36	0.08
1.5	−2.0	0.5		2.5	3.0	31 661.45	0.01
2.5	−2.0	0.5		3.5	3.0	31 662.76	−0.04
3.5	−2.0	0.5		4.5	3.0	31 663.77	−0.06
4.5	−2.0	0.5		5.5	3.0	31 664.46	−0.04
5.5	−2.0	0.5		6.5	3.0	31 664.80	−0.03
2.5	−3.0	0.5		3.5	4.0	31 665.85	−0.01
3.5	−3.0	0.5		4.5	4.0	31 666.91	0.00
4.5	−3.0	0.5		5.5	4.0	31 667.62	0.01
5.5	−3.0	0.5		6.5	4.0	31 667.96	0.00

[a] Only the K'' of $\Lambda = +1$ component is listed here. The actual wave function also contains $\Lambda = -1$ component with the sign of K'' opposite from the sign of K'' listed in the table. [b] J_1 and J_2 refer to the J quantum number of the spin–rotation component F_1 and F_2, respectively, which in turn corresponds to $J' = N' + {}^1/_2$ and $J' = N' - {}^1/_2$, respectively. Because the spin–rotation doublet of the $^2A_1$ state is not resolved and is considered to be degenerate, the transition frequency of $Q(J'',K'',F_1)$ and $R(J'',K'',F_1)$ is equal to that of $P(J'',K'',F_2)$ and $Q(J'',K'',F_2)$, respectively.

where N_E^T is the total population of the E state, Z is the rotational partition function, E_R is the energy of the specified rotational level calculated by eq 20 or some suitable approximation thereto, and g_I is the nuclear spin weight for a given rotational level (the $2J + 1$ rotational degeneracy is included in eq 29).

Weber[23] has considered the problem of nuclear spin weights for a number of symmetrical molecules. Using his reasoning, we deduce that the two components of the e rovibronic levels together have a nuclear spin statistical weight of 4, while the a_1 and a_2 levels which occur in pairs have a weight of 4 each. For CH_3O in the vibrationless level of the $\tilde{X}^2E$ state, we find that the rovibronic levels for which $P - \Sigma - \Lambda \neq 3m$ (m integer) are of e symmetry when $P - \Sigma - \Lambda = 3m$, one of the pair of functions defined by eq 4 is a_1, and the other is a_2, with the symmetries corresponding respectively to the plus and minus signs in that equation.

Programming eq 29, supplemented by eq 30, A14, and A14, allows us to predict all the spectral line intensities as a function of just one variable, the temperature T. Figure 1 shows a comparison of such a predicted and observed spectrum for the 0_0^0 transition. One can see that the agreement is very satisfactory assuming $T = 25$ K.

We have also simulated spectra taken from a continuous expansion. In those cases, lower temperatures (≈10 K) are required for the best fits, but here systematic discrepancies appear, indicating lack of Boltzmann equilibrium in these more intense expansions.

IV. Analysis and Results

The measured rotational transition frequencies for the vibrational bands assigned as 0_0^0 and 3_0^1 are given in Tables I and II, respectively. In section II, the theory of the energy levels of both the ground $\tilde{X}^2E$ and the $\tilde{A}^2A_1$ states has been worked out in considerable detail. In principle, then, one merely has to calculate the energy level differences as a function of the molecular parameters in the two states and "fit" the observed lines. This task is obviously made much easier by the existence of an excellent set of ground-state parameters from the work of Endo et al. However, we found that simply following this approach made assignments of warmer (≈20 K) spectra nearly impossible and even for our coldest spectra left a few unassigned lines. Moreover, the computational labor in such a direct approach is enormous if assignments do not "converge" very rapidly.

Therefore we developed the following iterative procedure. Two computer programs were written; one predicts transition frequencies from a set of molecular constants for both states; the other fits molecular constants from assigned methoxy line positions. To provide rapid turnaround time, it was desirable that these calculations be made in our laboratory computer (PC AT). Using the complete Hamiltonians of eq 20 and 27 would make this computation practically impossible. We therefore adopted a strategy of using eq 20 but neglecting all terms in the ground-state Hamiltonian, contained in $\mathcal{H}_3^R$, $\mathcal{H}_4^R$, $\mathcal{H}_D^{SR}$, and $\mathcal{H}_{CD}$. This approximation has the dramatic effect of making the ^2E state Hamiltonian 2×2 block diagonal, a problem easily handled by the PC AT. Furthermore, comparison of the ground-state energy level structure calculated in this manner as compared to the complete Hamiltonian, eq 20, revealed that almost all the shifts in energy were ≲10 MHz. For the microwave precision in the 0.01-MHz domain, eq 20 is absolutely necessary; for the optical accuracy of ≈1000 MHz, the above approximation clearly suffices.

With these two laboratory computer programs, the iterative analysis proceeded as follows. Analysis started with the coldest spectrum of the 3_0^1 band, which contained 17 distinct transitions of reasonable intensity. An initial assignment of seven lines was made by using combination differences and the ground-state energy levels predicted from the constants of Endo et al. These combination differences gave initial values for A' and B'. By iterating, predicting, and fitting, all but one line could be fit within experimental error.

It was then possible to proceed to warmer spectra. Finally some 47 lines were included in the analysis of the 3_0^1 band. By iterative procedure all were assigned; however, following the precedent of the coldest spectrum, six lines had residuals more than 5 times the expected experimental error. More to the point, these residuals were nearly constant. Since the upper state constants were now well determined, it became likely that there was apparently some small error in the ground-state energy levels.

It may seem surprising that an optical experiment with a precision roughly 10^5 lower than the microwave (and LMR) data would question the accuracy of the ground-state constants obtained from the latter. However, it must be remembered that several

(23) Weber, A. *J. Chem. Phys.* **1980**, *73*, 3952; **1981**, *74*, 4754; **1982**, *76*, 3694.

TABLE II: Methoxy $\tilde{A}^2A_1 \rightarrow \tilde{X}^2E_{3/2}$ 3_0^1 Rotational Transitions

J''	K''[a]	Σ''	J_1'[b]	J_2'[b]	K'	obsd, cm^{-1}	obsd − calcd
5.5	1.0	0.5	4.5		0.0	32 290.32	0.01
4.5	2.0	0.5	3.5		1.0	32 291.02	−0.01
5.5	0.0	0.5	4.5		1.0	32 293.77	0.06
4.5	1.0	0.5	3.5		0.0	32 294.58	0.04
3.5	2.0	0.5	2.5		1.0	32 294.94	0.05
3.5	3.0	0.5	3.5	2.5	2.0	32 295.74	0.08
4.5	2.0	0.5	4.5	3.5	1.0	32 296.87	−0.02
5.5	1.0	0.5	5.5	4.5	0.0	32 297.66	0.05
4.5	0.0	0.5	3.5		1.0	32 297.98	0.03
2.5	2.0	0.5	1.5		1.0	32 298.41	0.02
3.5	1.0	0.5	2.5		0.0	32 298.41	0.02
3.5	2.0	0.5	3.5	2.5	1.0	32 299.28	−0.01
4.5	1.0	0.5	4.5	3.5	0.0	32 300.45	0.06
5.5	0.0	0.5	5.5	4.5	1.0	32 301.09	0.05
2.5	2.0	0.5	2.5	1.5	1.0	32 301.34	0.02
2.5	1.0	0.5	1.5		0.0	32 301.91	0.03
3.5	1.0	0.5	3.5	2.5	0.0	32 302.82	0.04
4.5	0.0	0.5	4.5	3.5	1.0	32 303.76	−0.04
4.5	2.0	0.5	5.5	4.5	1.0	32 304.20	−0.02
2.5	1.0	0.5	2.5	1.5	0.0	32 304.86	0.04
1.5	1.0	0.5	0.5		0.0	32 305.00	−0.01
3.5	2.0	0.5	4.5	3.5	1.0	32 305.16	0.01
2.5	0.0	0.5	1.5		1.0	32 305.34	0.05
2.5	2.0	0.5	3.5	2.5	1.0	32 305.67	−0.04
3.5	0.0	0.5	3.5	2.5	1.0	32 306.21	0.01
1.5	1.0	0.5	1.5	0.5	0.0	32 306.44	−0.04
4.5	−1.0	0.5	4.5	3.5	2.0	32 307.11	−0.03
4.5	1.0	0.5	5.5	4.5	0.0	32 307.67	−0.05
2.5	0.0	0.5	2.5	1.5	1.0	32 308.24	0.02
3.5	1.0	0.5	4.5	3.5	0.0	32 308.62	−0.03
2.5	1.0	0.5	3.5	2.5	0.0	32 309.20	−0.02
1.5	1.0	0.5	2.5	1.5	0.0	32 309.35	−0.05
1.5	0.0	0.5	1.5	0.5	1.0	32 309.89	0.01
5.5	0.0	0.5	6.5	5.5	1.0	32 309.89	0.06
4.5	0.0	0.5	5.5	4.5	1.0	32 311.14	0.01
2.5	−1.0	0.5	2.5	1.5	2.0	32 311.51	−0.04
3.5	0.0	0.5	4.5	3.5	1.0	32 312.05	−0.01
0.5	0.0	0.5	1.5	0.5	1.0	32 312.66	0.03
1.5	0.0	0.5	2.5	1.5	1.0	32 312.75	−0.05
1.5	1.0	0.5		2.5	0.0	32 313.78	−0.02
4.5	−1.0	0.5	5.5	4.5	2.0	32 314.46	−0.01
2.5	1.0	0.5		3.5	0.0	32 315.04	−0.04
0.5	0.0	0.5		1.5	1.0	32 315.49	−0.07
3.5	1.0	0.5		4.5	0.0	32 315.94	−0.03
1.5	−1.0	0.5	2.5	1.5	2.0	32 316.04	−0.09
5.5	−2.0	0.5	6.5	5.5	3.0	32 316.47	0.02
4.5	1.0	0.5		5.5	0.0	32 316.47	−0.03
1.5	0.0	0.5		2.5	1.0	32 317.19	−0.01
4.5	−2.0	0.5	5.5	4.5	3.0	32 317.71	−0.02
2.5	.0	0.5		3.5	1.0	32 318.49	0.01
3.5	−2.0	0.5	4.5	3.5	3.0	32 318.62	−0.01
0.5	−1.0	0.5		1.5	2.0	32 318.90	0.02
2.5	−2.0	0.5	3.5	2.5	3.0	32 319.22	0.04
3.5	0.0	0.5		4.5	1.0	32 319.36	−0.02
1.5	−1.0	0.5		2.5	2.0	32 320.48	−0.05

[a] See footnote *a* of Table I. [b] See footnote *b* of Table I.

of the molecular parameters listed by Endo et al. are determined very indirectly. For example, there are no observed microwave transitions across the K stacks of the ground state. Indeed, the observed optical discrepancies could be accounted for easily by slightly shifting the relative position of the ^2E K stacks. In fact, variation of any one of several ^2E constants, e.g., A'', ϵ_{aa}, by an amount roughly 5–10 times its expected error limits, removed the observed discrepancies.

The question now was whether any combination of constants would fit the microwave and optical data simultaneously, within their respective experimental errors and, if so, what that combination would be. To resolve that question, one has to use the complete Hamiltonian of eq 20, including all the small terms. The resulting matrix is $(4J + 2) \times (4J + 2)$ with more than 20 variable parameters, a problem obviously requiring something beyond a personal computer.

Our approach was to use a nonlinear least-squares program running on the Cray at the Pittsburgh and then the Ohio Supercomputer Centers. The model was the differences in the assigned eigenvalues of the ^2E and $^2A_1$ states calculated from the Hamiltonians of eq 20 and 27.

For the least-squares fitting, a previously described program NLLSQ was used with modification on the Cray. The principal enhancement was to generalize the routine to handle quite different weights for the data points. The final weighting employed was 50 000:1 for the microwave data to optical data.

After the 3_0^1 band of methoxy was assigned, about 90 lines of the 0_0^0 band spectra were obtained by pulsed jet expansion. The procedure of calibration and assignment used was similar to that used for the 3_0^1 band. Since the spectra obtained in the pulsed jet are hotter than those obtained in the continuous-wave (cw) jet (~25 vs ~10 K), it is possible to determine the centrifugal constants of the $^2A_1$ state more accurately. Indeed, a comparison of the 2×2 nonlinear least-squares fitting of both the 0_0^0 and 3_0^1 bands showed that the $^2A_1$ state centrifugal constants of the 3_0^1 band were too large while the $^2A_1$ state rotational constants A

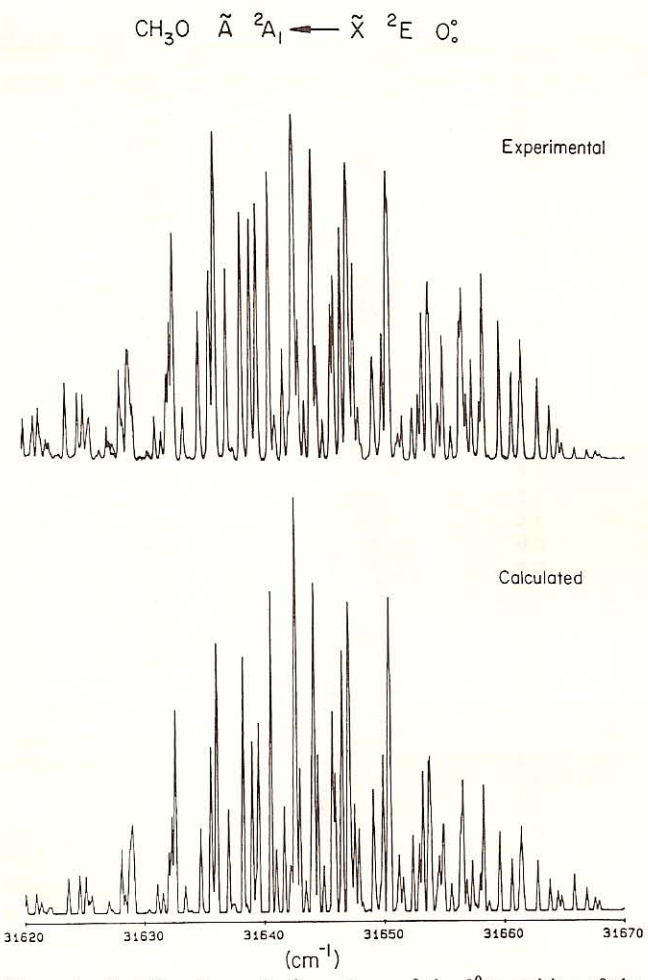

Figure 1. Rotationally resolved spectrum of the 0_0^0 transition of the methoxy radical. The upper trace shows the experimental spectrum, while the lower trace shows a simulation using eq 29 and assuming a rotational temperature of 25 K. The simulation is quite good but not perfect. The small discrepancies probably result from the approximations discussed in the text as well as possible small deviations from Boltzmann equilibrium among the rotational levels.

and B of both the 0_0^0 and 3_0^1 bands were in agreement with each other. This indicates that the centrifugal constants of 3_0^1 band obtained so far are not very reliable or, perhaps, some of the weak lines of 3_0^1 might even be misassigned. The same indications were obtained by the comparison of the $(4J + 2) \times (4J + 2)$ fittings with combining microwave spectra and 0_0^0, 3_0^1 optical spectra, respectively. The 3_0^1 band transitions were then reexamined, and it was found that just by changing the assignment of four lines on the lower frequency side of the spectrum and two lines on the higher frequency side, it was possible to get consistent contrifugal constants. All of those lines where the reassignment occurred are very weak.

The 0_0^0 band and the reassigned 3_0^1 band were then combined with the microwave transitions, and two microwave-optical $(4J + 2) \times (4J + 2)$ fittings were performed. A comparison of the constants obtained by these two fittings showed that, within 2 standard errors, the ^2E state constants were in agreement with each other. At this stage, it was desirable to combine the microwave and all the optical transitions together and carry out a joint fitting. The joint fitting was performed by assuming that both 0_0^0 and 3_0^1 bands have identical $^2A_1$ state centrifugal constants, and the final results are presented in Tables III and IV. It should be clearly noted that the quality of the fit to the microwave data is not degraded from that obtained by Endo et al. and there are no longer discrepancies within the residuals for the optical data. Of the major constants, i.e., those in the simple symmetric top model, only one has changed beyond the error limits given by Endo et al. That parameter is A'' (and perforce $A''\xi_t - \epsilon$), which has

TABLE III: CH_3O Molecular Parameters[a] (cm^{-1}) of the $\tilde{X}^2E$ Ground State

	ref	
	b	this work
$a\xi_e d$	−62.24 (17)	−61.974 (70)
A''	5.169 (19)	5.2059 (36)
B''	0.931 683 (15)	0.931 6825 (7)
$A''\xi_t - \epsilon$	1.812 (9)	1.7730 (36)
ϵ_{aa}	1.365 (57)	−1.3533 (40)
ϵ_{bc}	$-4.76\ (22) \times 10^{-2}$	$-4.35\ (11) \times 10^{-2}$
$\epsilon_{2a}{}^c$	$8.07\ (360) \times 10^{-2}$	$8.092\ (14) \times 10^{-2}$
$\epsilon_2 1$	$-5.7263\ (127) \times 10^{-3}$	$-5.7359\ (40) \times 10^{-3}$
h_1	$2.5166\ (59) \times 10^{-3}$	$2.5117\ (17) \times 10^{-3}$
h_2	$4.663\ (133) \times 10^{-2}$	$4.605\ (47) \times 10^{-2}$
$\eta_K\xi_t$	$4.400\ (604) \times 10^{-3}$	$4.400 \times 10^{-3}{}^e$
$\eta_e\xi_t$	$6.1\ (31) \times 10^{-5}$	$6.1 \times 10^{-5}{}^d$
D''_N	$2.519\ (15) \times 10^{-6}$	$2.519 \times 10^{-6}{}^d$
D''_{NK}	$2.568\ (13) \times 10^{-5}$	$2.568 \times 10^{-5}{}^d$
D''_K	$7.03 \times 10^{-5}{}^e$	$7.03 \times 10^{-5}{}^e$
h_{1N}	0.0^e	0.0^e
h_{1K}	$7.86\ (39) \times 10^{-6}$	$7.86 \times 10^{-6}{}^d$
h_{2N}	$-1.6\ (14) \times 10^{-7}$	$-1.6 \times 10^{-7}{}^d$
h_{2K}	$-1.74\ (16) \times 10^{-5}$	$-1.78\ (43) \times 10^{-5}{}^d$
h_4	$6.3\ (46) \times 10^{-8}$	$6.3 \times 10^{-8}{}^d$
$a_D\xi_e d$	$4.5\ (25) \times 10^{-3}$	$3.48\ (86) \times 10^{-3}$
$E(^2E_{3/2}, K{=}0, J{=}0.5)$		−3.105 (100)

[a] 2.5 times standard error in parentheses. [b] Endo, Y.; Saito, S.; Hirota, E. *J. Chem. Phys.* **1984**, *81*, 122. [c] $\epsilon_{2b} = \epsilon_{2a}B''/A''$. [d] Fixed at value in footnote *b*. [e] Fixed.

TABLE IV: CH_3O Molecular Parameters[a] (cm^{-1}) for the $\tilde{A}^2A_1$ State

$\nu_{00} = 31\,614.513\ (39)$	$\nu_{10} = 32\,276.866\ (43)$
$A'_0 = 4.9810\ (34)$	$A_1' = 4.9833\ (67)$
$B'_0 = 0.742\,67\ (57)$	$B_1' = 0.732\,52\ (136)$
$D'_N = 2.519 \times 10^{-6}{}^b$	$D'_N = 2.519 \times 10^{-6}{}^b$
$D'_{NK} = 2.568 \times 10^{-5}{}^b$	$D'_{NK} = 2.568 \times 10^{-6}{}^b$
$D'_K = 7.04 \times 10^{-4}{}^b$	$D'_K = 7.04 \times 10^{-4}{}^b$

[a] 2.5 times standard error in parentheses. [b] Held at ground-state value.

shifted by about 5 standard deviations. Interestingly, some of the minor parameters have adjusted fairly significantly to "conform" to the new A'' value. In addition, many of the error limits have changed significantly with the addition of the optical data.

Table IV gives the molecular parameters for the $\tilde{A}^2A_1$ state which are determined for the first time by this experiment. These are given for the vibrationless level and $v'_3 = 1$.

In addition, the rotational analysis establishes an extremely precise value for methoxy's band origin, i.e., $T_{00} = 31\,614.51\ cm^{-1}$. It is worth noting, as is done in Table III, that with use of the conventional definitions, the lowest level (the $^2E_{3/2}$, $K = 0$, $J = 0.5$ level) of each vibrational state lies below the band origin. For the vibrationless level, this difference amounts to $-30.11\ cm^{-1}$, yielding an excitation frequency from this lowest level of $31\,644.62\ cm^{-1}$.

It is interesting to compare the geometries of methoxy in its $\tilde{X}$ and $\tilde{A}$ states. Unfortunately, there are three structural parameters, the C–H and C–O bond distances and the HCH bond angle, while there are only two rotational constants, A and B, determined for each state. (At this point we neglect the small Jahn–Teller geometric distortion represented by h_1 and h_2.) We have isotopic data for CD_3O, but without the corresponding microwave data for CD_3O, it would be very difficult to disentangle the ground- and excited-state rotational constants. (See note added in proof.)

We are thus forced to make a geometric assumption about methoxy. Carbon–hydrogen bonds vary little over a wide variety of compounds. Thus we will assume that methoxy and methanol have equivalent C–H bond lengths. 1.10 Å, within an uncertainty of 0.02 Å. Table V is built upon that assumption and gives the corresponding HCH bond angle and CO bond length. Probably the most interesting observation (and one least likely to be affected by the C–H bond length assumption) concerns the change in

TABLE V: CH_3O Geometry[a]

parameter	state $\tilde{X}^2E$	state $\tilde{A}^2A_1$
R_{CH}, Å	1.10 ± 0.02	1.10 ± 0.02
R_{CO}, Å	1.37 ± 0.02	1.58 ± 0.02
∠HCH, deg	109 ± 3	113 ± 4

[a] The C–H bond length is assumed (based upon CH_3OH and related molecules) to be 1.10 Å in both states with an uncertainty of 0.02 Å. This uncertainty, which is the dominant uncertainty, is propagated into the other bond length and angle.

geometry between the ground and excited state.

As can be seen from Table V, the CO bond lengthens by over 0.2 Å between these two states. Such a lengthening had been presaged by the significant drop in the CO stretching frequency in the $\tilde{X}$ and $\tilde{A}$ states. It is also qualitatively consistent but larger than that predicted by a previous ab initio calculation.[12] However, this work represents the first experimental determination of high precision for the excited $\tilde{A}$ state geometries and hence the first true measure of the change in geometry between the states. While less dramatic, Table V also clearly shows that the HCH bond angle clearly opens up (by ≈4°) in going to the excited $\tilde{A}$ state.

Besides the rotational constants, Table III also lists a number of parameters, e.g., h_1, h_2, $a\xi_e d$, etc., more or less directly related to the Jahn–Teller effect in methoxy. Our values for these parameters do not vary qualitatively from those previously reported by Endo et al. They discussed the implications of these parameters at some length, but clearly several questions remain unanswered. We will defer further discussion of these parameters until our analysis of the vibronic structure of the Jahn–Teller active modes is complete. Hopefully, a combination of all the Jahn–Teller related parameters will yield a complete picture of the distortion of this molecule.

Acknowledgment. We gratefully acknowledge the support of the National Science Foundation for this work under Grant CHE 8507537 and grants of computer time from the Ohio and Pittsburgh Supercomputer Centers.

Appendix

Equation 29 contains two factors $S_{ab}(\alpha,\beta)$ and $S_{bc}(\beta,\gamma)$. Since in our experiment, both a and c correspond to the ^2E ground state of methoxy and b corresponds to the excited $^2A_1$ state, we shall adopt the notation $S_{ca}(\alpha,\beta)$ and $S_{ae}(\beta,\gamma)$. Because of the Hermitian nature of the matrix elements involved so long as $\alpha = \gamma$, if we calculate S_{ca}, S_{ae} can be obtained from it trivially.

We now need to consider explicitly the quantum numbers associated with α and β. For the ^2E ground state the case-a-like basis functions can be written following eq 4 as

$$|E,J,P,M,S,\Sigma,\pm\rangle = 2^{-1/2}[|\Lambda=1,J,P,M,S,\Sigma\rangle \pm (-1)^{J-P+S-\Sigma}|\Lambda=-1,J,-P,M,S,-\Sigma\rangle] \quad \text{(A1)}$$

Thus we associate with α the quantum numbers exhibited in the ket on the left-hand side of eq A1. Following eq 25 and 26 we can write the $\tilde{A}$ state case-b-like basis functions as

$$|A,J,M,N,K,S,\pm\rangle = \sum_{M_S,M_N} (-1)^{N-S+M}(2J+1)^{1/2} \times \begin{pmatrix} N & S & J \\ M_N & M_S & -M \end{pmatrix} |N,K,M_N,\pm\rangle|SM_S\rangle \quad \text{(A2)}$$

Thus we associate with β the quantum numbers exhibited in the ket on the left-hand side of eq A2.

In order to compute S_{ea}, it is useful to express the case b functions in terms of case a functions, i.e.

$$|A,J,M,N,K,S,\pm\rangle = \sum_{P,\Sigma}(-1)^{-J+P+2S}(2N+1)^{1/2}\begin{pmatrix} J & N & S \\ P & -K & -\Sigma \end{pmatrix}|A,J,P,M,S,\Sigma,\pm\rangle \quad \text{(A3)}$$

Because $S = {}^1/_2$, there are only two terms in this sum, so one can write explicitly

$$|A,J,M,N,K,S,p\rangle = C_1(J,K,\delta)|A,J,P=K+\Sigma,M,S,\Sigma,p\rangle + C_2(J,K,\delta)|A,J,P=K-\Sigma,M,S,-\Sigma,p\rangle \quad \text{(A4)}$$

where

$$C_1(J,K,\delta) = \left[\frac{J \mp K + {}^1/_2}{2J+1}\right]^{1/2} \quad \text{(A5a)}$$

$$C_2(J,K,\delta) = \mp\left[\frac{J \pm K + {}^1/_2}{2J+1}\right]^{1/2} \quad \text{(A5b)}$$

$\delta = 1$ or 2, corresponding respectively to the spin components F_1 ($N = J - {}^1/_2$) or F_2 ($N = J + {}^1/_2$), respectively. In eq A5 the top signs correspond to F_2 and the lower to F_1. The p takes on the parity quantum number values plus aand minus. For the special case of $K = 0$, the case b basis function reduces to

$$|A,J,M,N,K=0,S,p\rangle = |A,J,P=\Sigma,M,S,\Sigma,\pm\rangle \quad \text{(A6)}$$

where the only state existing for N even is the plus case a state of symmetry A_1 and for N odd the minus case a state of symmetry A_2.

We can now consider the line-strength function $S_{ae}(\alpha,\beta)$ in isotropic space for the $K \neq 0$ case:

$$S_{ae}(\alpha,\beta) = 3\sum_{MM'}|\langle\alpha|\mu_z|\beta\rangle|^2 = 3\sum_{M,M'}|C_1(J,K,\delta)\langle E,J,P,M,S,\Sigma,p|\mu_z|A,J',P'=K'+\Sigma',M',S,\Sigma',p'\rangle + C_2(J,K,\delta)\langle E,T,P,M,S,\Sigma,p|\mu_z|A,J',P'=K'-\Sigma',M',S,-\Sigma',p'\rangle|^2 \quad \text{(A7)}$$

To simply eq A7, it is worthwhile considering in detail the case a matrix elements. Let us define

$$\mu_a(\alpha,\beta) = \langle E,J,P,M,S,\Sigma,p|\mu_z|A,J',P',M',S,\Sigma',p'\rangle \quad \text{(A8)}$$

μ_z corresponds to the 0th component of a first-rank irreducible tensor operator in the space-fixed coordinate system which is related to the corresponding quantities $T^1_r(\mu)$ in the molecule fixed system by

$$\mu_z = \sum_r D^1_{0r}(\omega)\ T^1_r(\mu) \quad \text{(A9)}$$

where $\mathbf{D}^1$ is the rotational matrix relating through the Euler angles, ω, the molecule-fixed and space-fixed system. We can now write

$$\mu_a(\alpha,\beta) = \sum_r\langle E,J,P,M,S,\Sigma,p|D^1_{0r}(\omega)\ T^1_r(\mu)|A,J',P',M',S,\Sigma',p'\rangle = (-1)^{-M}[(2J+1)(2J'+1)]^{1/2}\begin{pmatrix} J & 1 & J' \\ M & 0 & M' \end{pmatrix}\times \left[(-1)^P\begin{pmatrix} J & 1 & J \\ -P & 1 & P' \end{pmatrix}\langle E(\Lambda=1)|T^1_1(\mu)|A(\Lambda=0)\rangle + pp'(-1)^{J+J'-P-P'}\langle E(\Lambda=-1)|T^1_{-1}(\mu)|A)\Lambda=0)\rangle\right](-1)^{-P}\begin{pmatrix} J & 1 & J \\ P & -1 & -P' \end{pmatrix} \quad \text{(A10)}$$

The matrix elements in eq A10 are quadratures over the vibronic eigenfunctions corresponding to a specific vibrational level of the ^2E and $^2A_1$ electronic states. For an A–E transition in C_{3v} symmetry, the $r = 0$ term in the summation vanishes, leaving only the $r = \pm 1$ terms. The product pp' yields a plus sign if the ± symmetry of the ^2E and $^2A_1$ states are the same and a minus sign if they are different. The "cross terms" between the two-component basis functions vanish because the electric dipole moment operator is zero between states with different values of Σ. Likewise, the matrix elements $\langle E(\Lambda=\pm1)|T^1_{\mp1}(\mu)|A(\Lambda=0)\rangle$ vanish, because they are not invariant under the symmetry operation C_3.

If we now insert the results of eq A10 into eq A7 for $S_{ae}(\alpha,\beta)$ and perform the sum over M, utilizing the properties of the 3 – j symbols, we obtain

$$S_{ae}[(E,J,P,\Sigma,p),(A,J,N,K,P')] - \frac{(-1)^{2J}}{2}(2J'+1)(2J+1)\times$$
$$\left\{C_1(J,K,\delta)\left[\langle E(\Lambda=1)|T^1_1(\mu)|A(\Lambda=0)\rangle(-1)^P\begin{pmatrix} J & 1 & J' \\ -P & 1 & P'-K+\Sigma\end{pmatrix} + pp'(-1)^{J+J'-P-P'}\langle E(\Lambda=-1)|T^1_{-1}(\mu)|A(\Lambda=0)\rangle(-1)^{-P}\times \begin{pmatrix} J & 1 & J' \\ P & -1 & -P'=-K-\Sigma\end{pmatrix}\right] + p'(-1)^{J'-P'+S+\Sigma}C_2(J,K,\delta)\times$$
$$\left[\langle E(\Lambda=1)|T^1_1(\mu)|A(\Lambda=0)\rangle(-1)^P\begin{pmatrix} J & 1 & J' \\ -P & 1 & P'=-K+\Sigma\end{pmatrix} + pp'(-1)^{J-J'+P'-P-2\Sigma}\langle(\Lambda=1)|T^1_1(\mu)|A(\Lambda=0)\rangle(-1)^{-P}\times \begin{pmatrix} J & 1 & J' \\ P & -1 & P'=K-\Sigma\end{pmatrix}\right]\right\}^2 \quad \text{(A11)}$$

To simplify $S_{ae}(\alpha,\beta)$ further, we must use the relationship

$$\langle E(\Lambda=1)|T^1_1(\mu)|A(\Lambda=0)\rangle = -\langle E(\Lambda=-1)|T^1_{-1}(\mu)|A(\Lambda=0)\rangle \quad \text{(A12)}$$

Equation A12 follows from the facts that under the symmetry operation σ_v (for methoxy reflection in the plane containing one hydrogen and bisecting the H–C–H angle formed by the other two hydrogens), as shown by Hougen[24]

$$\sigma_v|E(\Lambda=\pm1)\rangle = +E|(\Lambda=\mp1)\rangle \quad \text{(A13a)}$$

$$\sigma_v T^1_{\pm1}(\mu) = -T^1_{\mp1}(\mu) \quad \text{(A13b)}$$

It is clear that in eq A11 the $3-j$ symbols multiplying respectively $C_1(J,K,\delta)$ and $C_2(J,K,\delta)$) cause at a maximum only one of the two terms to be nonvanishing for any value of K. In addition from eq A5 $|C_1(J,K,\delta)| = |C_2(J,-K,\delta)|$, so we obtain

$$S_{ae}[(E,J,P,\Sigma,p),(A,J',N,K\neq0,\gamma,p')] = \delta_{p,-p'}(2J+1)[J'+(-1)^\delta(\Sigma-P)+(-1)^\delta+\tfrac{1}{2}]\times |\langle E(\Lambda=1)|T^1_1(\mu)|A(\Lambda=0)\rangle|^2\begin{pmatrix} J & 1 & J' \\ -P & 1 & P'=K+\Sigma\end{pmatrix}^2 \quad \text{(A14)}$$

where as before $\delta = 1$ or 2 corresponding to the F_1 and F_2 components of the $\tilde{A}$ state and for the $^2E_{3/2}$ state $\Sigma = {}^1/_2$ while for the $^2E_{1/2}$ state $\Sigma = -{}^1/_2$. $S_{ae}(\alpha,\beta)$ may also be seen to vanish unless the states connected differ in the parity quantum number p.

For the case of $K = 0$, the expression for $S_{ae}(\alpha,\beta)$ can be derived analogously:

$$S_{ae}[(E,J,P,\Sigma,p),(A,J',N,K=0,\gamma,p')] = (2J+1)(2J'+1)|\langle E(\Lambda=1)|T^1_1(\mu)|\Lambda=0\rangle|^2\times \begin{pmatrix} J & 1 & J' \\ -(1+\Sigma) & 1 & \Sigma\end{pmatrix}^2 \quad \text{(A15)}$$

(24) Hougen, J. T. *J. Chem. Phys.* **1962**, *37*, 1433; **1963**, *39*, 358.

where now for each N there is either a plus or a minus combination, not both.

If one inserts eq A14 (or eq A15) into eq 29, then one has a complete formula for the intensity. It should be noted that in eq 29 the last S factor, representing the emission process, is to be summed over all the quantum numbers of the (final) E state. The quantum numbers J, P, Σ, and p are explicit in eq A14 (or eq A15), and the sum is easily performed by using the properties of the $3-j$ symbols. However, there is one sum, contained in the vibronic matrix element $|\langle E(\Lambda=1)|T^1_1(\mu)|A(\Lambda=0)\rangle|^2$, that requires summing over all "vibrational" levels of the ^2E "electronic" state to which emission occurs.

This sum reduces to a constant that does not vary significantly under the following three assumptions: (i) All transitions from the excited $\tilde{A}$ state terminate on totally symmetric vibrational levels of the $\tilde{X}$ state. Our previous observations[7] of the resolved emission spectrum of CH_3O indicate that when pumping 0^0_0 or 3^0_0 more than 80% of the emission terminates upon the totally symmetric vibrational levels. (ii) The vibronic transition moment can be factored into a Franck–Condon factor and an electronic transition moment. This is true for the totally symmetric vibrational levels of CH_3O which are only weakly affected by the Jahn–Teller interactions. (iii) As indicated in eq 29, the frequency dependence of the detector and the ν_f^3 can be taken as constant. This assumption allows the summation of the Franck–Condon factor to unity. While the methoxy emission spectrum is extended, its range is not so great as to introduce serious errors with this approximation.

Finally, eq A14 and A15 are derived for the ideal situation of the ^2E state being exactly case a and the $^2A_1$ state being exactly case b. In actual practice, the deviation of the A state is unobservable experimentally. For the E state the deviation is small but observable. Strictly speaking, the state characterized by $|E,J,P,M,S,\Sigma,\pm\rangle$ should be replaced by the corresponding eigenfunction

$$|E,J,P,M,S,\Sigma,\pm\rangle' = \sum_{q,\sigma} Q_{q,\sigma}|E,J,q,M,S,\sigma,\pm\rangle \quad \text{(A16)}$$

where q runs from $-J$ to J and $\sigma = \pm{}^1/_2$. The $Q_{q,\sigma}$ coefficients are obtained from the numerical diagonalization of the ^2E state matrix, and we find $Q_{P,\Sigma} \approx 1$ always and only three other coefficients are ever nonnegligible, i.e., $Q_{P-2\Sigma,-\Sigma}$, $Q_{-P+2+2\Sigma,\Sigma}$, and $Q_{-P+2,-\Sigma}$. The values of S_{ae} actually used in eq 30 of the text were numerically calculated via eq A14–A17, including all four of these coefficients.

Note Added in Proof. Using the B rotational constants of $^{13}CH_3O$ and $^{12}CD_3O$ from a recent paper (Momose, T.; Endo, Y.; Hirota, E.; Shida, T. *J. Chem. Phys.* **1988**, *88*, 5338) and A and B constants of $^{12}CH_3O$ in the present paper, the $\tilde{X}^2E$ state geometry of methoxy is determined as $r_{CH} = 1.106$ Å, $r_{CO} = 1.363$ Å, and $\angle HCH = 108.3°$.

Registry No. CH_3O, 2143-68-2.